Noise and Vibration: *Emerging Methods*
NOVEM 2009
5-8 April 2009 Oxford

A REVIEW OF STABILIZED FEM FOR HELMHOLTZ EQUATION

Hadrien Beriot* and Michel Tournour

LMS International,
Interleuvenlaan 68, Researchpark Z1,
3001 Leuven, Belgium
Email: hadrien.beriot@lmsintl.com

ABSTRACT

One major bottleneck of the Galerkin FE approach for solving Helmholtz equation is the so-called pollution effect. For large scale problems, when the dimensions of the domain become significant when compared to the wavelength, the well known "rule of thumb" which consists in using 8 to 10 points per wavelength, can yield notable errors. In practice, it is often unaffordable to increase the discretization. To tackle this general issue, many researchers have tried to implement more sophisticated basis, using physics based interpolation for instance. However, for industrial applications, the standard low order polynomial approach is still appropriate due to its flexibility and excellent conditioning properties. Therefore, some efforts have also been made to reduce the dispersion of the standard method, without radically modifying the existing programs. Using dispersion analysis, we first compare the different approaches. Then 3D applications on unstructured meshes are presented, showing very significant improvement of the FE solution at a negligible extra computational cost.

1 INTRODUCTION

It is well known that the numerical resolution of wave problems presents a very specific problem called dispersion. In fact, everything happens as if the sound velocity in the discrete domain was slightly different from the one in the continuous domain: the original dispersion relation is not respected and method is said to be dispersive. For a given level of discretization, let's say 10 points per wavelength, global error is not controlled when the frequency increases because phase error tends to accumulate. Dispersion errors is the main reason for the so-called pollution effect which represents the major drawback of standard FE methods for wave propagation, as it limits their use to the low frequency applications. It can be shown that for linear 1D finite element on a regular mesh of length h the following relation holds [1]:

$$\kappa^h = \pm\frac{1}{h}\arccos\left(\frac{6-2\left(\kappa h\right)^2}{6+\left(\kappa h\right)^2}\right), \tag{1}$$

where κ is the original wave number and κ^h is the numerical wave number. This well known result indicates that if condition $\kappa^h h \geq \sqrt{12}$ is satisfied (which represents approximately 1.81 points per wavelength) κ^h is real valued and the numerical solution is non dissipative. In every cases, the system is obviously dispersive, κ^h does not verify the original dispersion relation $\kappa = \omega/c_0$, where

ω is the angular velocity and c_0 is the sound velocity. By a Taylor series expansion, it can be shown that [1]:

$$\kappa^h - \kappa = -\frac{\kappa^3 h^2}{24} + \mathcal{O}(\kappa^5 h^4). \tag{2}$$

The widely used "rule of thumb" in engineering applications consists in using 6 to 10 points per wavelength to obtain satisfactory results. This rule, by keeping κh constant indeed guarantees a good local error, but it cannot help to control the global error when κ increases. Due to the dispersion, the $\kappa^3 h^2$ term has to be kept constant, which means that the number of points per wavelength should be enlarged with increasing values of κ. Unfortunately, this option enhances significantly the computational cost, making the medium and high-frequency applications prohibitively expensive.

To tackle this general issue, very different directions were proposed. Many researchers tried to modify radically the standard FEM by enriching [2] or even replacing the polynomial approximation space by wave-based functions [3, 4] which verify the correct dispersion relation. These methods, however, present two main drawbacks: their resulting system matrix potentially suffers from severe ill-conditioning and they are efficient on applications of moderate geometrical complexity. Yet, the simplicity and flexibility of low order polynomial approximations, widely used in the industrial context, still offer substantial benefits. Consequently, efforts have also been made over the last two decades to reduce the phase error of standard methods, without radically modifying the existing programs. Among the numerous publications, two promising directions can be distinguished.

The first approach, originally proposed by Harari and Hugues [5] is the so-called Galerkin least squares (GLS) approach. The idea is to append to the standard Galerkin formulation a residual in least squares form. This added term is multiplied by a stability parameter which must be properly defined. Using linear elements, the GLS approach simply leads to modifying the sound celerity in the discrete domain, in order to locally compensate the error on the numerical phase. It can be easily realized from Equation (1) that the dispersion error can be fully eliminated in a one dimensional analysis. As dispersion generally varies according to the wave orientation, the dispersion error cannot be completely removed for higher dimensions [1], but it can be significantly reduced [6]. Though these schemes are designed for structured grids, numerical experiments prove that substantial improvements can be reached on highly distorted meshes [7].

The second approach has been proposed by Guddati and Yue [8]. Using dispersion analysis, they prove that the phase error on quadrilateral elements can be tremendously reduced only by slightly under-integrating the mass and stiffness matrices. The most remarkable aspect of such modified quadrature rules is that it leads to a fourth-order asymptotic behavior of the dispersion error, which has to be compared to the second order rate of standard Galerkin or Galerkin least squares. It is also demonstrated numerically that the method applies well to non structured meshes.

More recently, Thompson and Kunthong [9] made a significant advance on the topic by unifying these two approaches under the theoretical framework of Generalized Galerkin least squares (GGLS) methods. Optimal GGLS stabilization parameters is proved to be closely related to special quadrature rules. In particular, for quadrilateral and hexahedral elements, the schemes of reference [8] are exactly retrieved. Considering various mesh stencils, quadrature rules for triangles and tetrahedrons are provided through numerical dispersion analysis.

The objective of this paper is to test the benefits of stabilized FEM on a real-life 3D engineering problem. As parabolic elements are less subject to dispersion [2], we will only focus on the stabilization of linear elements. Special attention is also devoted to the conditioning properties of the resulting system matrix, of utmost importance for iterative solvers performance.

This paper is organized as follows. In section 2, the different formulations are presented. In Section 3 a dispersion analysis is performed on distorted quadrangles in order to compare the dispersion error of the GLS and the GGLS approach. In the last section, a three dimensional benchmark is performed on a realistic engineering case.

2 FORMULATIONS

In this section, a survey of the different stabilization techniques is proposed. The Galerkin least squares, the modified integration rules and the Generalized Galerkin least squares approaches are briefly reviewed.

2.1 Galerkin

The time harmonic acoustics problem is governed by the Helmholtz equation. It aims at finding the acoustic pressure perturbation p on a domain Ω such that:

$$(\Delta + \kappa^2)p = -s \tag{3}$$

where function s represents the amplitude of a time harmonic source term. In general, a Robin boundary condition is applied on the surfaces of the domain Γ, defined by:

$$\frac{\partial p}{\partial n} + \gamma p = g, \text{ on } \Gamma \tag{4}$$

where g and γ are functions of space and wavenumber. Domain Ω is partitioned into finite elements and a Galerkin variational approach is applied to Equation (3). It consists in finding $p^h \in H^1(\Omega)$ such that:

$$A(q^h, p^h) = F(q^h), \quad \forall q^h \in H^1(\Omega), \tag{5}$$

with the sesquilinear form:

$$A(q^h, p^h) = \int_\Omega \nabla q^h \cdot \nabla p^h \, d\Omega - \kappa^2 \int_\Omega q^h p^h \, d\Omega + \int_\Gamma \gamma q^h p^h \, d\Gamma \tag{6}$$

and the source term:

$$F(q^h) = \int_\Omega q^h s \, d\Omega + \int_\Gamma q^h g \, d\Gamma. \tag{7}$$

2.2 Galerkin least squares (GLS)

Among the techniques for reducing dispersion error at a low implementation cost, the Galerkin least squares approach (GLS) outstands. In the GLS method, a least squares operator is added to the Galerkin formulation (5) as follows:

$$A(q^h, p^h) + B(q^h, p^h) = F(q^h), \quad \forall q^h \in H^1(\Omega). \tag{8}$$

This additional operator is constructed from a residual r^h of the governing equation (3) evaluated within element interiors:

$$B(q^h, p^h) = \int_\Omega \tau(\Delta q^h + \kappa^2 q^h) \, r^h \, d\Omega, \tag{9}$$

where:

$$r^h = (\Delta p^h + \kappa^2 p^h) - f. \tag{10}$$

In this expression, τ is a local ponderation parameter with units of inverse length squared. Obviously if $\tau = 0$, GLS reverses to Galerkin formulation. Considering linear elements, all second order derivatives vanish and formulation (8) simply leads to:

$$\int_\Omega \nabla q^h \cdot \nabla p^h - \kappa^2 \phi \, q^h p^h \, d\Omega + \int_\Gamma \gamma q^h p^h \, d\Gamma = \phi \int_\Omega q^h s \, d\Omega + \int_\Gamma q^h g \, d\Gamma, \tag{11}$$

where the non dimensional quantity $\phi = (1 - \tau\kappa^2)$ is to be determined through dispersion analysis. It could be remarked that if parameter τ is taken spatially constant, solving (11) is equivalent to solving (5) with an artificially shifted frequency. Unfortunately, phase error is anisotropic and cannot be eliminated along whole directions. The following expression:

$$\phi = \frac{6}{(\kappa h)^2} \frac{1 - \cos(\kappa h)}{2 + \cos(\kappa h)}, \tag{12}$$

noted GLS(0) is often used. It eliminates the phase error of plane waves aligned with the grid ($\theta = 0$), in uniform meshes of quadrangle linear element. However, dispersion along the diagonal ($\theta = \pi/4$) will be very important and it is generally recommended to use GLS$(\pi/8)$ [6]. The GLS approach can be generalized to non uniform meshes through a proper definition of the local h value in relation (12) (for instance $h = \sqrt{S}$, where S is the element area). Numerical evidence show that the GLS can still yield significant improvements on highly distorted meshes [7].

2.3 Modified quadrature rules

The dispersion analysis is a well known tool that has been extensively studied for Helmholtz equation [10]. The originality of the approach of Guddati and Yue [8] lies in the fact that they incorporate the quadrature rules explicitly in their analysis. By doing so, they prove that the dispersion error can be dramatically improved simply by slightly shifting the gauss points in the mass and stiffness operators integration. Consider a regular infinite mesh of quadrangle elements as plotted in Figure 1.

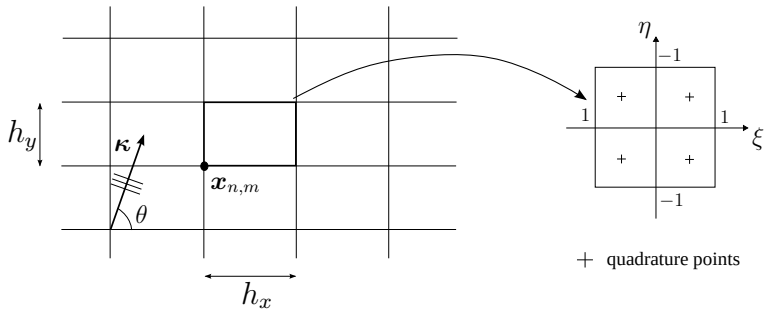

Figure 1. Cartesian periodic mesh for dispersion analysis.

In the absence of source term ($s = 0$), the discretization of the Helmholtz Galerkin formulation (5) will lead to a system of the form:

$$Dp^h = 0, \tag{13}$$

where D is an infinite matrix and p^h is a vector containing all nodal unknowns. In practice, all finite elements on the grid are mapped from a reference element $(\{-1 < \xi < +1\} \times \{-1 < \eta < +1\})$ on which the integration is performed. This integration is traditionally evaluated using the following four points Gauss quadrature rule $(\xi = \pm\alpha; \eta = \pm\alpha)$ for a unitary weight, where $\alpha = 1/\sqrt{3}$. The coefficient matrix for a four node rectangular finite element of size $h_x \times h_y$ is given by [8]:

$$S = \begin{bmatrix} S_0 & S_x & S_{xy} & S_y \\ S_x & S_0 & S_y & S_{xy} \\ S_{xy} & S_y & S_0 & S_x \\ S_y & S_{xy} & S_x & S_0 \end{bmatrix}, \tag{14}$$

where:

$$S_0 = \frac{(h_x^2+h_y^2)(\alpha^2+1)}{4h_xh_y} - \frac{h_xh_y}{16}(1+\alpha^2)^2\kappa^2,\ S_x = \frac{(h_x^2-h_y^2)-\alpha^2(h_x^2+h_y^2)}{4h_xh_y} - \frac{h_xh_y}{16}(1-\alpha^4)\kappa^2,$$
$$S_y = \frac{(h_y^2-h_x^2)-\alpha^2(h_x^2+h_y^2)}{4h_xh_y} - \frac{h_xh_y}{16}(1-\alpha^4)\kappa^2,\ S_{xy} = \frac{(h_x^2+h_y^2)(\alpha^2-1)}{4h_xh_y} - \frac{h_xh_y}{16}(1-\alpha^2)^2\kappa^2.$$

Due to the mesh periodicity, all nodes in the grid verify the same form of equation. If $p^h_{n,m}$ denotes the pressure at node (n,m), after the assembly of all elementary matrices (14), it can be shown that all lines of the system (13) result in:

$$\begin{aligned} &4S_0p^h_{n,m} + 2S_x(p^h_{n-1,m} + p^h_{n+1,m}) + 2S_y(p^h_{n,m-1} + p^h_{n,m+1}) \\ &+S_{xy}(p^h_{n-1,m-1} + p^h_{n+1,m-1} + p^h_{n+1,m+1} + p^h_{n-1,m+1}) = 0. \end{aligned} \tag{15}$$

Assuming that the solution at nodes is a plane wave of the form:

$$p^h(\boldsymbol{x_{n,m}}) = \exp(\mathrm{i}\boldsymbol{\kappa^h}\cdot\boldsymbol{x_{n,m}}) \tag{16}$$

with $\boldsymbol{\kappa^h} = \kappa^h(\cos\theta, \sin\theta)$, yields the following expression:

$$[S_0 + S_xC_x + S_yC_y + S_{xy}C_xC_y] = 0, \tag{17}$$

where $C_x = \cos(\kappa^h h_x\cos\theta)$ and $C_y = \cos(\kappa^h h_y\sin\theta)$. Equation (17) represents the discrete model dispersion relationship. Taking the Taylor expansion of κ in terms of κ^h the dispersion error can be written as [8]:

$$\left|\frac{\kappa-\kappa^h}{\kappa^h}\right| = \frac{\kappa^2}{24}\left|(3\alpha^2-2)(h_x^2+h_y^2)\cos^2\theta\sin^2\theta + (2-3\alpha^2)(h_x^2\cos^2\theta h_y^2\sin^2\theta)\right| + \mathcal{O}(\kappa^4(h_x+h_y)^4). \tag{18}$$

From this expression it is clear that standard integration rules yield a second order accuracy of the phase error. Yet, a simple shift of the quadrature points to the unconventional locations of:

$$(\xi = \pm\sqrt{2/3}; \eta = \pm\sqrt{2/3}) \tag{19}$$

corresponding to $\alpha^2 = 2/3$ suppresses the leading error term and yields a fourth order accuracy. Another remarkable property of this approach is that contrary to GLS, the stabilization process is not frequency dependent. As a consequence, the modified quadrature rules can be used for time harmonic response as well as for eigenmodes computations.

2.4 Generalized Galerkin least squares

In a recent article Thompson and Kunthong [9], explored the framework of the Generalized Galerkin least squares (GGLS). The GGLS consists in linear combining the GLS formulation with another least squares operator involving the gradient residual, as follows:

$$A(q^h,p^h) + B(q^h,p^h) + C(q^h,p^h) = F(q^h) \tag{20}$$

with:

$$C(q^h,p^h) = \int_\Omega \nabla(\Delta q^h + \kappa^2 q^h)\cdot\overline{\overline{\sigma}}\,\nabla r^h\,d\Omega. \tag{21}$$

The originality of their approach lies in the optimal design of the stabilization parameters τ and $\overline{\overline{\sigma}}$, which are taken independent of the frequency and the mesh size h. Instead, these parameters are defined in terms of the spatial position on the reference element, through a Taylor-series of the discrete dispersion relation very similar to the one described in 2.3. In fact, this approach can

be seen as a mathematical framework for the rather intuitive modified integration rules approach. In the absence of source terms, it can be proved that optimal GGLS for rectangular elements is strictly equivalent to performing quadrature (19).

To derive new integration rules for triangles and tetrahedral elements, Thompson and Kunthong define specific cyclically repeatable stencils. For the triangle, a 7 node stencil of 6 equilateral elements is used and for the tetrahedron, they implement a patch of 20 equilateral elements forming a 13 point stencil. If the design of the quadrature rules is optimal for these stencils, the improvement for other stencils and/or distorted meshes is questionable. However, numerical evidence on 2D test cases show that the dispersion error reduction on unstructured meshes is still significant.

3 DISPERSION ANALYSIS

The GLS and GGLS are optimally designed for regular periodic meshes. Their behavior on such grids is well documented, optimal GGLS is known to yield a 4^{th} order phase accuracy, while GLS keeps the standard 2^{nd} order. However there is little knowledge on how the mesh distortion really affects their performance. For this reason, a special numerical dispersion analysis has been performed.

3.1 Description of the method

Consider a standard mesh pattern of four quadrangles and apply increasing perturbations to the central node position, yielding the four mesh stencil given in Figure 2. Stencil #1 is taken as a reference, the central node is not perturbed and mesh is regular. Let's now copy these stencils and translate them of a length $2h$ in the two directions to form an infinite mesh, as illustrated in Figure 3.

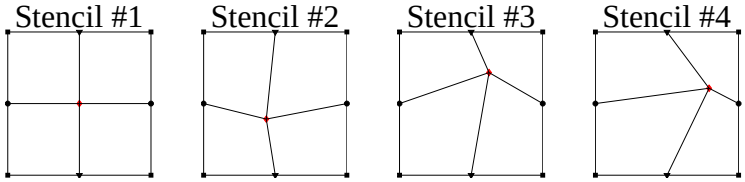

Figure 2. Different mesh stencils used for the dispersion analysis.

Dispersion analysis is presented in Section 2.3 on a regular mesh for the Galerkin formulation and the methodology can be followed closely to derive the GLS and GGLS phase errors of stencil #1. However, for the three other stencils, the mesh is not regular and the dispersion analysis requires more attention to be derived.

Heuristically, from Figure 3, we can easily isolate four types of nodes ($N_t = 4$) on the perturbed stencils. These nodes are located at the same cyclically repeating locations and the full mesh can be represented just by copying and translating them. All the nodes belonging to the same type form what we will call a patch. On each patch j, we assume that the solution at node of coordinate $\boldsymbol{x}$ takes the form:

$$p_j^h(\boldsymbol{x}) = \varphi_j \exp(\mathrm{i}\boldsymbol{\kappa^h} \cdot \boldsymbol{x}), \quad j = 1, \cdots, N_t. \tag{22}$$

Due to the mesh structure, every node of a given patch verifies the same form of equation in system (13). Substituting (22) in each of these equations will yield a new linear system on the wave amplitudes of the form:

$$R(\omega, \kappa^h)\varphi = 0, \tag{23}$$

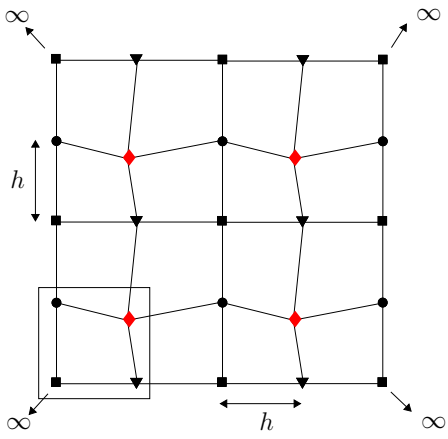

Figure 3: Translation invariant mesh used for the dispersion analysis. The four different types of node are represented with dedicated markers.

with $\varphi = (\varphi_1, \varphi_2, \cdots, \varphi_{N_t})^T$. This system represents the dispersion relation of the discrete numerical problem. By finding values of κ^h verifying (23), we are able to compute the dispersion error, defined as:

$$E_d = 100 \times \left| \frac{\kappa^h - \kappa}{\kappa} \right|. \tag{24}$$

3.2 Results

To validate our approach, we first present results obtained on the unperturbed mesh stencil #1. The dispersion error is plotted on figure 4 as a function of the propagation angle for two different discretization levels, $n_\lambda = 6$ and $n_\lambda = 10$. For obvious symmetry reasons, θ varies only from 0 to $90°$.

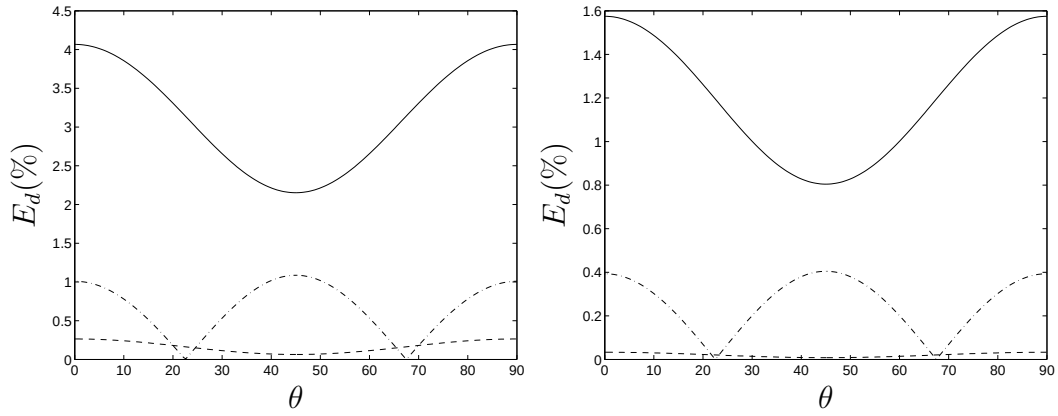

Figure 4: Dispersion errors on the mesh stencil #1 with $n_\lambda = 6$ (left) and $n_\lambda = 10$ (right). Solid line: Galerkin; dashed line: GGLS; dashed dotted line: GLS ($\pi/8$).

The phase error strongly depends on the propagation angle. For standard Galerkin, dispersion is maximum when the wave propagates along the mesh grid and minimum when the wave propagates diagonally across the mesh. Note that increasing the resolution reduces the error but does not change the level of anisotropy: there is still a factor 2 between the best and worst directions. As mentioned in Section 2.2, the GLS was parameterized with an angle of $\pi/8$. For that specific angle, dispersion is completely annihilated and GLS cannot be beaten. However, excepted in the close vicinity of that angle, the optimal GGLS formulation (or equivalently the modified

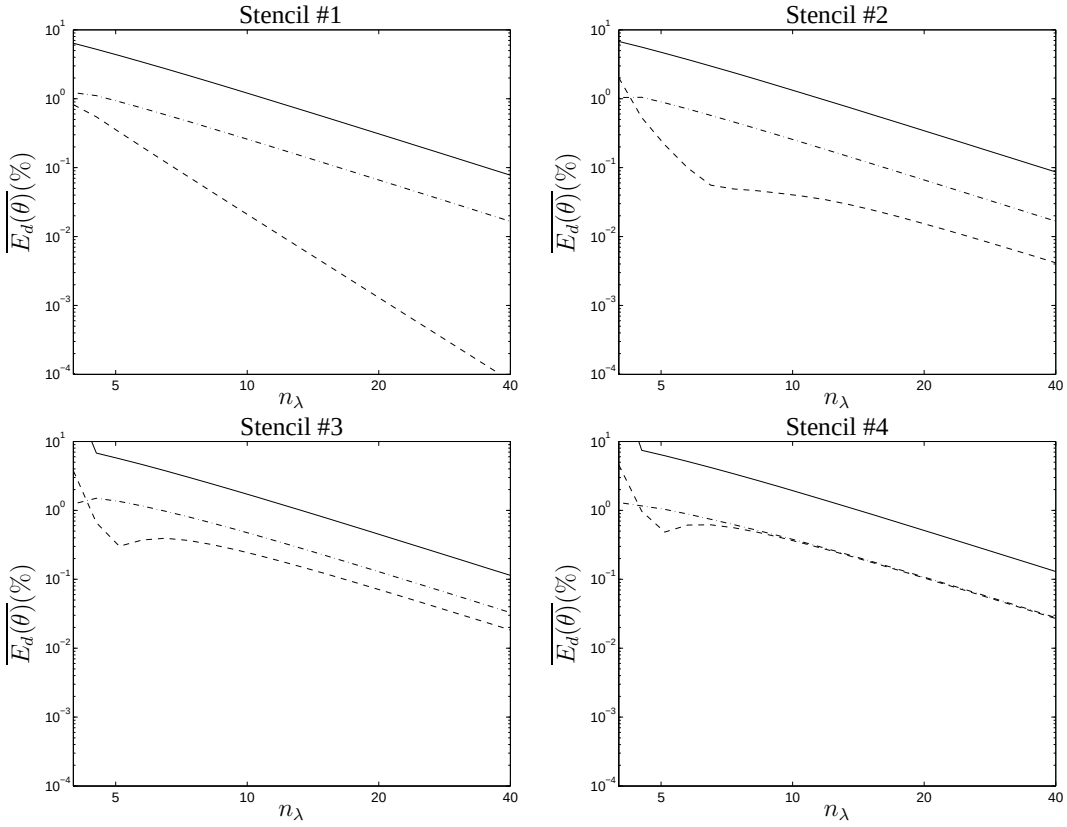

Figure 5: Dispersion error as a function of the discretization level. Solid line: Galerkin; dashed line: GGLS; dashed dotted line: GLS ($\pi/8$).

integration rules approach) clearly outperforms the GLS formulation. At the somehow underestimated level of discretization $n_\lambda = 6$, the GGLS formulation is as dispersive as a $n_\lambda = 20$ Galerkin scheme.

Consider now the dispersion error as a function of the discretization level. The dispersion error is averaged over the whole unit circle ($\theta \in [-\pi, \pi]$) and we perform computations for the four mesh stencils on the range $n_\lambda = [4, 40]$. Results are displayed in figure 5. Stencil #1 is in perfect accordance with previously published materials:

- Phase error convergence is of 2^{nd} order for Galerkin.
- GLS divides by 10 the phase error while keeping a 2^{nd} order convergence rate.
- GGLS outperforms and presents a 4^{th} order convergence rate.

The results on the three other stencils are very instructive:

- The mesh distortion does not dramatically alters the Galerkin and GLS performance. 2^{nd} order accuracy is still obtained and GLS still improves significantly the phase error.
- GGLS rapidly looses its super-convergence rate to retrieve a 2^{nd} order rate. In spite of that, this method still offer substantial benefits over GLS for the stencils 2 and 3.

These results clearly highlight the superiority of the GGLS over the GLS. Even though no 4^{th} order convergence rate should be expected on a distorted mesh, the stabilization effect is still very effective.

4 NUMERICAL VALIDATION

The objective of this section is to test the benefits of the GGLS formulation on a realistic engineering problem. The geometry chosen corresponds to a small car compartment, which cavity size is approximately $2.75m \times 1.6m \times 1.20m$ (seats are not modeled). Two different meshes will be used (see figure 6), their specifications and spectrum validity (with a rule of thumb of 8 points per wavelength) are presented in Table 1.

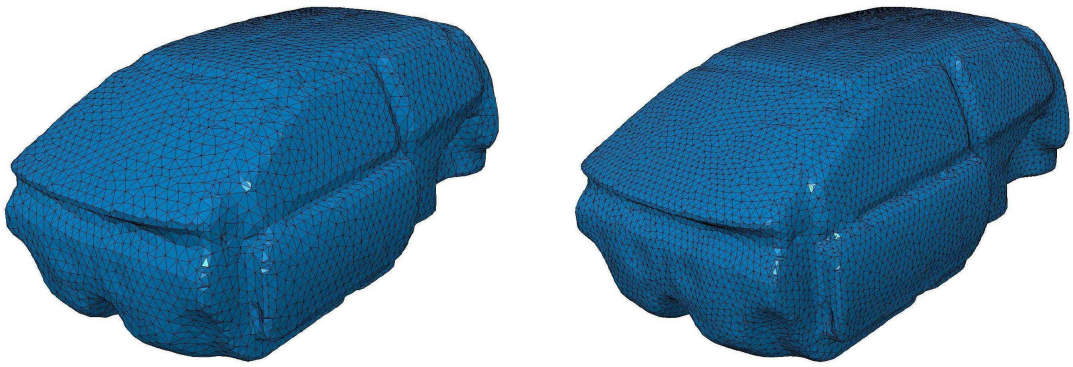

Figure 6. Car compartment mesh #1 (left) and mesh #2 (right).

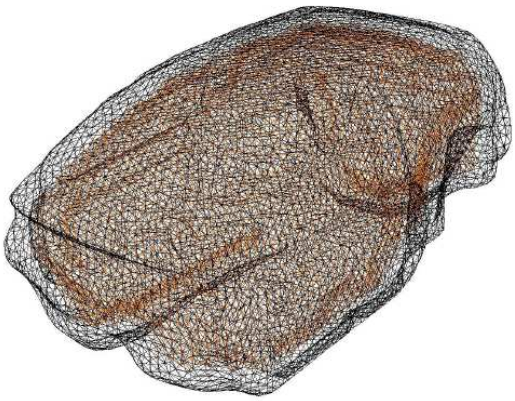

Figure 7: Detail of mesh #1. The hexaedral elements appear in brown color, tetrahedral elements appear in black.

Mesh	#1	#2
Number of nodes	24000	92000
Number of H8 elements	13000	67000
Number of T4 elements	52000	143000
Mesh validity ($n_\lambda \approx 8$)	< 500 Hz	< 1000 Hz

Table 1. Mesh specifications

The two meshes are “hybrid”, they contain tetrahedral (T4) and hexaedral (H8) elements, as visible in Figure 7. Mesh #2 will be used as a reference for both problems, knowing that it is considered reliable up to approximately 1000 Hz. We first perform a modal analysis, to study the benefits of the stabilization on the eigenvalues accuracy. Then we focus on a direct computation

and compare the sound pressure levels (SPL) at passenger's ears for a source placed inside the cavity.

4.1 Modal analysis

One remarkable aspect of the GGLS approach of Thompson and Kunthong [9], is that the parameters are not frequency dependent. Consequently, the stabilization can also be used for eigenmode computations. In Figure 8, we present a comparison between the eigenfrequencies obtained via the Galerkin and the GGLS formulations on mesh #1. The eigenvalues obtained with Galerkin on the mesh #2 are also depicted as a reference.

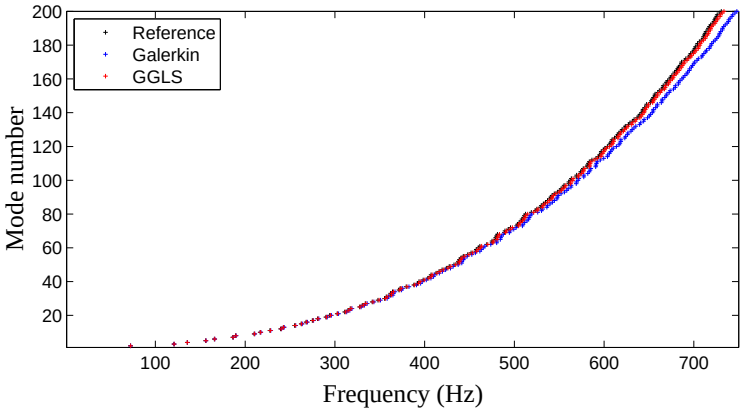

Figure 8. Representation of the 200 first eigenfrequencies of the car compartment model.

At low frequency, the mode patterns are still "slowly" oscillating and the phase errors are not consequent. Thus, up to the validity limit of mesh #1 corresponding more or less to the 70^{th} mode, the gain is relatively low. However, at higher frequencies the improvement is impressive. To further highlight the effect of stabilization, the frequency shift for each mode is depicted in Figure 9, showing the progressive deviation of the Galerkin formulation which tends to overestimate the model rigidity. The stabilized scheme corrects this unfavorable aspect, it is still able to provide reliable eigenvalues much below the recommended discretization level. On mode 200 with only around six points per wavelength, the GGLS solver deviates of approximately 3 Hz, whereas the Galerkin solver is overestimating the frequency of nearly 20 Hz.

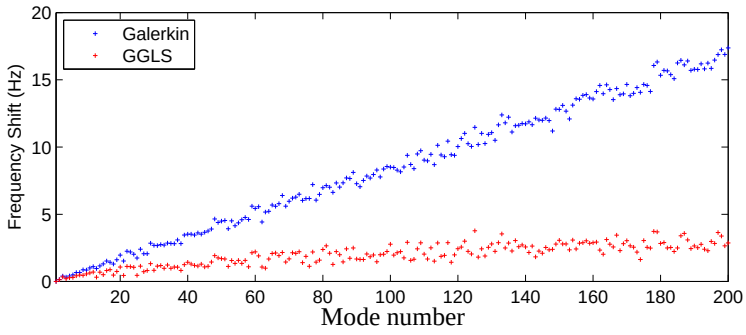

Figure 9. Frequency shift for each mode.

4.2 Forced response

Consider now a forced response configuration. A monopole source is placed at the back of the car. Regarding the boundary conditions, an absorbing panel is applied at the roof with constant impedance $Z = 600 - 6000\mathrm{i}$, the complementary panels being considered rigid.

Results for mesh #1 are evaluated on the range $[300, 600]$ Hz with a 0.5 Hz step. We present in Figure 10 the response function at a point located near the driver's ear. The blue curve represents the Galerkin response and the red curve the GGLS response. As a reference, a Galerkin computation was made on the refined mesh #2, represented by the black curve. The GGLS scheme clearly achieves better accuracy. Above 300 Hz with actual FEM, the resonances are shifted to upper values and solution becomes quickly unreliable, whereas stabilized scheme provides an excellent accuracy up to 600 Hz.

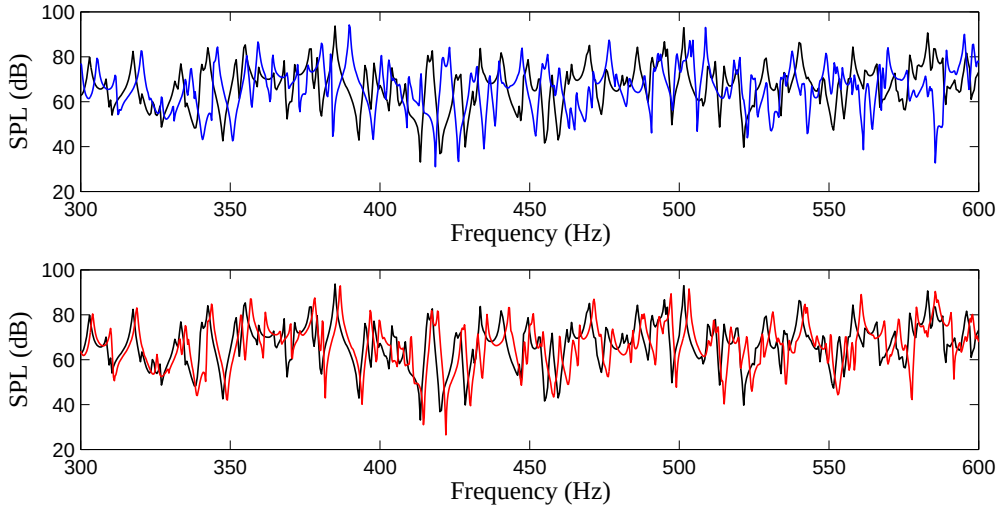

Figure 10: Comparison of SPL at passenger's ears. Black line: reference solution; Blue line: Galerkin solution; Red line: GGLS solution

It is also crucial to assess the conditioning properties of the GGLS system matrix, knowing that any deterioration of the condition number may strongly affect the performance of iterative solvers [11]. We compare in Table 2 the condition numbers of the GGLS and the Galerkin system

Frequency (Hz)	100	300	600
Galerkin	1.41×10^4	0.86×10^4	1.18×10^4
GGLS	5.52×10^4	3.66×10^4	2.26×10^4

Table 2. Condition number of system matrix for mesh #1

matrix for various frequencies on mesh #1: the two system conditioning are very similar for this test case. Though further studies are required, this example seems to prove that the computational cost of GGLS is virtually equivalent to Galerkin.

5 CONCLUSION

In this paper, different stabilization techniques to reduce the phase errors on Helmholtz FEM were reviewed. Through a dispersion analysis, we examined the effect of the grid distortion on the performance of both GLS and optimized GGLS. We proved that although no super-convergent behavior should be expected on distorted grids, the GGLS is clearly outstanding. A realistic 3D engineering case was then performed to test the stabilization effect on both eigenmode and direct response applications. The GGLS optimized formulation showed results invariably superior and to a considerable margin to standard Galerkin, at virtually no extra computational cost.

Acknowledgment

The work presented in this paper has been performed in the framework of the ongoing project IWT-070337 “MIDAS next generation numerical tools for mid-frequency acoustic”, which is supported by IWT Vlaanderen.

REFERENCES

[1] I. Babuska and S.A. Sauter. Is the pollution effect of the fem avoidable for the helmholtz equation considering high wavenumbers? *SIAM Journal of Numerical Analysis*, 34:2392–2423, 1997.

[2] M Ainsworth. Discrete dispersion relation for *hp*-version finite element approximation at high wave number. *SIAM Journal of Numerical Analysis*, 42(2):553–575, 2004.

[3] C. Farhat, I. Harari, and L.P. Franca. The discontinuous enrichment method. *Computer methods of Applied Mechanics in Engineering*, 48, 2001.

[4] T. Huttunen, P. Monk, and J.P. Kaipio. Computational aspects of the ultra weak variational formulation. *Journal of Computational Physics*, 182:27–46, 2002.

[5] I. Harari and T.J.R. Hughes. Galerkin/least squares finite element method for the reduced wave equation with non-reflecting boundary conditions. *Computational methods in Applied Mechanics and engineering*, 98:411–454, 1992.

[6] L. Thompson and P.M. Pinsky. A Galerkin least squares finite element method for the two dimensional Helmholtz equation. *International Journal for numerical methods in engineering*, 38:371–397, 1995.

[7] I Harari and F. Magoules. Numerical investigations of stabilized finite element computations for acoustics. *Wave Motion*, 39:411–454, 2003.

[8] M.N. Guddati and B. Yue. Modified integration rules for reducing dispersion error in finite element methods. *Computer methods in applied mechanics and engineering*, 193:275–287, 2004.

[9] L. Thompson and P. Kunthong. A residual based variational method for reducing dispersion error in finite element methods. *Proceedings of IMECE*, 32, 2005.

[10] A. Deraemaeker, I. Babuska, and P. Bouillard. Dispersion and pollution of the FEM solution for the Helmholtz equation in one, two and three dimensions. *International Journal for Numerical Methods in Engineering*, 46:471–499, 1999.

[11] Anne Greenbaum. *Iterative Methods for Solving Linear Systems*. Frontiers in applied Mathematics, 1997.